Acta Crystallographica Section B
Structural Science, Crystal Engineering and Materials
ISSN 2052-5206

High-pressure-induced structural changes, amorphization and molecule penetration in MFI microporous materials: a review

Giovanna Vezzalini, Rossella Arletti and Simona Quartieri

Acta Cryst. (2014). B**70**, 444–451

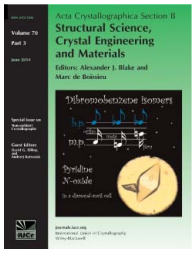

Acta Crystallographica Section B: Structural Science, Crystal Engineering and Materials publishes scientific articles related to the structural science of compounds and materials in the widest sense. Knowledge of the arrangements of atoms, including their temporal variations and dependencies on temperature and pressure, is often the key to understanding physical and chemical phenomena and is crucial for the design of new materials and supramolecular devices. *Acta Crystallographica B* is the forum for the publication of such contributions. Scientific developments based on experimental studies as well as those based on theoretical approaches, including crystal-structure prediction, structure–property relations and the use of databases of crystal structures, are published.

Acta Crystallographica Section B
Structural Science, Crystal Engineering and Materials
ISSN 2052-5206

High-pressure-induced structural changes, amorphization and molecule penetration in MFI microporous materials: a review

Giovanna Vezzalini,[a]* Rossella Arletti[b] and Simona Quartieri[c]

[a]Dipartimento di Scienze Chimiche e Geologiche, Università di Modena e Reggio Emilia, via S. Eufemia 19, 41100 Modena, Italy, [b]Dipartimento di Scienze della Terra, Università di Torino, Via Valperga Caluso 35, 10125 Torino, Italy, and [c]Dipartimento di Fisica e Scienze della Terra, Università di Messina, Viale Ferdinando Stagno d'Alcontres 31, 98166 Messina S, Italy

Correspondence e-mail: mariagiovanna.vezzalini@unimore.it

Received 6 November 2013
Accepted 10 April 2014

This is a comparative study on the high-pressure behavior of microporous materials with an MFI framework type (*i.e.* natural mutinaite, ZSM-5 and the all-silica phase silicalite-1), based on *in-situ* experiments in which penetrating and non-penetrating pressure-transmitting media were used. Different pressure-induced phenomena and deformation mechanisms (*e.g.* pressure-induced over-hydration, pressure-induced amorphization) are discussed. The influence of framework and extra-framework composition and of the presence of silanol defects on the response to the high pressure of MFI-type zeolites is discussed.

1. MFI materials

Zeolites are microporous materials which are used in an impressive range of applications. In particular, those with MFI-framework type (Baerlocher *et al.*, 2001) have wide industrial interest as shape-selective catalysts, selective absorbers and have recently been used in nano-electronics and nano-sensoring. Different natural and synthetic phases exhibit this structure: the rare natural zeolite mutinaite (Galli *et al.*, 1997; Vezzalini *et al.*, 1997) and several synthetic phases, as ZSM-5 (Kokotailo *et al.*, 1978; Olson *et al.*, 1981) and the pure-silica silicalite (Artioli *et al.*, 2000; Flanigen *et al.*, 1978).

The unique structure of MFI porous materials consists of intersecting channels formed by rings of 10 $(Al,Si)O_4$ tetrahedra (10MR), obtained by the linking of five-membered rings chains. The channels are linear in the *b* direction (Fig. 1) and sinusoidal in the *ac* plane. The window openings of 10MR have a diameter of 5–6 Å, which enables compounds of comparable size to enter and diffuse into the channels. The chemical composition of these materials is very variable, both in the framework and in the extra-framework content. The Si/Al ratio, strictly related to the extraframework content (cations and water molecules), defines the degree of hydrophobicity of the material and can range from about seven in the natural mutinaite (hydrophilic phase) to infinite in the pure-silica silicalite (highly hydrophobic). In mutinaite, the Al/Si substitution is balanced by solvated alkaline and earth alkaline cations in the channels. In silicalite, the zeolite pores are nearly empty, due to the lack of heteroatom substitutions in the framework, and only few H_2O molecules are usually present. In synthetic ZSM-5 a variable number of cations can be located in the channels, depending on the extent of Al/Si substitution.

ZSM-5 was originally synthesized in the presence of a specific organic template (tetrapropylammonium cation; Argauer & Landolt, 1972) and was presented as a significant example of the need for large organic cations to crystallize zeolites with low aluminium content. Later, MFI-type zeolites

were produced using a large variety of organic molecules (Lok *et al.*, 1983) and, finally, the synthesis of Na-ZSM-5 in the absence of any organic molecule confuted the established theories (Cundy & Cox, 2003; Flanigen *et al.*, 1978).

The maximum topological symmetry of MFI phases is orthorhombic (space group *Pnma*), but often the general symmetry is reduced to monoclinic due to several factors: the nature and amount of Si substituents, extra-framework content and distribution, temperature and pressure (de Vos Burchart *et al.*, 1993; Hay & Jaeger, 1984). In particular, a reversible monoclinic ($P2_1/n$)/orthorhombic (*Pnma*) phase transition is induced in ZSM-5 and silicalite-1 by temperature, as a result of the relative shift of (010) pentasil layers in the *c* direction (van Koningsveld *et al.*, 1987; Fig. 1). In silicalite-1 this transition occurs at about 320 K, while the presence of aluminium in the framework of ZSM-5 lowers this temperature. For $SiO_2/Al_2O_3 < 110$, the transition occurs below room temperature (Hay & Jaeger, 1984), indicating that an MFI zeolite with this composition is orthorhombic at ambient conditions.

2. Microporous materials under pressure

Recently it has been demonstrated that besides high temperature, high pressure (HP) can also induce important structural changes in zeolites, modifying the accessibility of the catalytic sites, the physical and chemical properties and, consequently, their possible applications.

Most of the studies on zeolites under pressure have been performed by *in situ* X-ray/neutron powder and single-crystal diffraction (see for reviews Arletti *et al.*, 2003; Gatta, 2008; Leardini *et al.*, 2010; Ori *et al.*, 2008), IR/Raman spectroscopy (Belitsky *et al.*, 1992; Goryainov, 2005; Goryainov & Smirnov, 2001; Goryainov *et al.*, 1996, 2003; Huang, 1998; Miroshnichenko & Goryainov, 2000), mercury porosimetry, ^{1}H and ^{29}Si MAS NMR spectroscopy and calorimetric studies (Desbiens *et al.*, 2005; Karbowiak *et al.*, 2010; Trzpit *et al.*, 2007, 2008), and by theoretical methods (see, for example, Betti *et al.*, 2007; Demontis *et al.*, 2003; Fois, Gamba, Tabacchi, Quartieri *et al.*, 2005; Sartbaeva *et al.*, 2006, 2012).

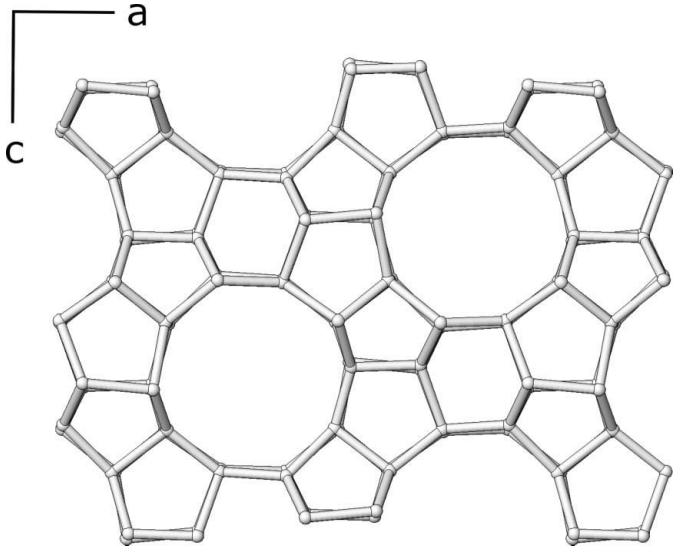

Figure 1
Projection of the MFI framework along [010], showing the straight 10MR channels running parallel to the *b* axis.

In the experimental HP studies of zeolites, either 'pore penetrating' or 'non-penetrating' pressure-transmitting media (PTM) are used. The former are usually aqueous/alcohol mixtures, whose molecular sizes are small enough to penetrate the zeolite pores (see Ori *et al.*, 2008 for a review); the latter are usually silicone oil or glycerol, formed by molecules too large to penetrate (see *e.g.* Arletti *et al.*, 2010, 2011; Fois *et al.*, 2008; Gatta, 2005; Leardini *et al.*, 2010, 2012, 2013; Quartieri *et al.*, 2011, 2012).

The peculiar characteristic of the zeolite structures, built by rigid tetrahedral units, is that the main deformation mechanism under HP is controlled by tetrahedral tilting and the structural rearrangement at HP is mainly driven by framework geometry and symmetry. Moreover, the studies performed with 'non-penetrating' media highlighted the crucial influence of the framework type and composition, and of the extra-framework content on the zeolite response to pressure, in terms of deformation mechanisms and compressibility (Arletti *et al.*, 2003; Fois, Gamba, Tabacchi, Arletti *et al.*, 2005; Gatta, 2005, 2008; Leardini *et al.*, 2010, 2012, 2013). The zeolite compressibility derived by experiments using non-penetrating PTM does not appear directly related to the material porosity, expressed as 'framework density' (FD; Baerlocher *et al.*, 2001), but strictly related to the nature, radius and valence of the extra-framework cations, and to the number of H_2O molecules. As a consequence, some zeolites, although characterized by large pores, can be unexpectedly less compressible than other Si-pure phases with empty cavities, and other denser silicates. This specific role has been clearly confirmed by systematic investigations on fibrous (Gatta, 2005), CHA (Leardini *et al.*, 2010, 2012, 2013) and MFI (Arletti *et al.* 2011; Quartieri *et al.*, 2011, 2012) framework topologies, working on materials with the same framework type but different extra-framework and framework compositions.

The use of 'penetrating' media has been exploited in different pressure regimes, to test different effects on the microporous-media systems. It is known that compressing a zeolite with an aqueous solution can induce the so-called pressure-induced hydration (PIH) effect (Lee *et al.*, 2004), which consists of the penetration of additional H_2O molecules into the zeolite channels in response to the applied pressure. This phenomenon – which usually occurs from ambient conditions to about 3 GPa (Ori *et al.*, 2008) – is particularly interesting with the irreversibility of the process upon pressure release, since in this case a new material with different composition and possible different properties is produced. Over-hydration of zeolites has usually been obtained using highly hydrostatic water–alcohol mixtures as PTM at pressures of the order of a few GPa. In zeolites of the fibrous family (Lee *et al.*, 2002; Likhacheva *et al.*, 2006, 2007; Seryotkin *et al.*, 2005) the PIH induces an abrupt volume

expansion, as a consequence of the penetration of additional H_2O molecules in new extraframework sites. On the contrary, in gismondine (Ori *et al.*, 2008), boggsite (Arletti *et al.*, 2010) and NaA (Likhacheva *et al.*, 2006), PIH occurs without cell volume expansion, due to the new water molecules in already existing extra-framework sites, or as a consequence of the presence of very large 12-ring channels like in zeolites Y (Colligan *et al.*, 2004) and LTL (Lee *et al.*, 2007).

Beyond PIH, occurring at pressures of the order of a few GPa, another phenomenon has attracted renewed interest in recent years: H_2O condensation in hydrophobic all-silica zeolites, a process that occurs at pressures of the order of a few MPa (see *e.g.* Cailliez *et al.*, 2008; Demontis *et al.*, 2003; Desbiens *et al.*, 2005; Trzpit *et al.*, 2007). Understanding the changes in water structure and dynamics as a consequence of interactions with confining surfaces is of paramount interest to advances in fundamental sciences and several technological applications (*i.e.* inhibition of corrosion, heterogeneous catalysis, design of super-hydrophobic surfaces, biological membranes, water purification). Specifically, interest in the confinement of water to nanoscopic spaces, like zeolitic cavities, stems from the fact that the properties of confined water are believed to be very different from those of the bulk fluid. In particular, understanding the changes in water properties when the confining surfaces are hydrophobic is relevant, for instance, in the selective adsorption processes where all-silica zeolites or activated C atoms are used (for example, for water purification; Eissmann & LeVan, 1993; Stelzer *et al.*, 1998). To penetrate liquid water in a hydrophobic microporous matrix, a certain pressure must be applied (Washburn, 1921). In general, different behaviors, exemplified by isothermal pressure/volume diagrams, can be observed, depending on various physical parameters of the matrix, such as pore size, pore system, dimensionality of the channels (one-, two- or three-dimensional; Fadeev & Eroshenko, 1997; Martin *et al.*, 2002; Trzpit *et al.*, 2009*a*,*b*) and on the hydrophobic/hydrophilic character of the zeolite (Trzpit *et al.*, 2007, 2008).

According to the reversible or irreversible character of the intrusion–extrusion cycle, the 'water–Si zeolite' systems are able to restore, absorb or dissipate mechanical energy. Consequently, molecular 'spring', 'damper' or 'shock-absorber' behavior can be observed (Cailliez *et al.*, 2009; Eroshenko *et al.*, 2001, 2002; Soulard *et al.*, 2004; Trzpit *et al.*, 2009*a*,*b*).

Not only water condensation inside zeolite cavities has attracted interest in recent years, but also the hyper-confinement of other guest molecules. It has been demonstrated, in fact, that the confinement of organic molecules (*e.g.* ethylene) inside zeolite channels can induce polymerization reactions. The application of pressure (in some cases enhanced by UV light irradiation) is the most efficient means to reduce intermolecular distances (Santoro *et al.*, 2013) and has the great advantage of avoiding the use of catalysts and radical initiators generally used for the synthesis of these materials (Chelazzi *et al.*, 2004; Citroni *et al.*, 2002; Schettino & Bini, 2003).

The compression of zeolites using non-penetrating media or in the absence of a medium (that is in non-hydrostatic conditions) is used to induce another phenomenon, the so-called pressure-induced amorphization (PIA; Havenga *et al.*, 2003; Huang, 1998; Huang & Havenga, 2001; Lui *et al.*, 2001; Richet & Gillet, 1997; Rutter *et al.*, 2000, 2001; Secco & Huang, 1999; Sharma & Sikka, 1996). PIA is observed, often after a transition to a structurally related crystalline phase, for a wide range of silicate structures and is characterized by important volume reduction, leading to a new material denser than the crystalline and the glass phases. The amorphization can be a reversible or irreversible transformation and it is extremely sluggish when compared with the thermal-induced transitions.

The first works on PIA of porous materials were carried out on fibrous zeolites by Belitsky *et al.* (1992) and Gillet *et al.* (1996) which found an amorphization pressure of ~ 12 GPa. Greaves *et al.* (2003) explored the time dependence and dynamics of zeolite amorphization generated by compression and found evidence for polyamorphism. This consists of the coexistence of different amorphous phases with the same composition but different densities. These authors determined that a more ordered and lower density amorphous phase (LDA) is formed at the onset of the collapse, and a higher density, more disordered phase (HDA) is formed by successive compression. Many papers, both experimental and theoretical, demonstrate a strict dependence of the amorphization pressure and its reversibility on the zeolite composition (Huang & Havenga, 2001; Gulín-González & Suffritti, 2004; Arletti *et al.*, 2003). In particular, for a certain zeolite, PIA is irreversible in the presence of extra-framework small cations (*e.g.* H) and reversible for larger ones (*e.g.* Li and Na). The same rationale also applies to the role of water molecules, which contrast PIA (Fois, Gamba, Tabacchi, Arletti *et al.*, 2005; Peral & Iñiguez, 2006).

This paper reviews the high-pressure behavior of MFI microporous materials, dividing the discussion into the following sections: elastic behavior and compressibility, pressure-induced hydration and molecule intrusion and amorphization processes. Notwithstanding the strong interest raised in the zeolite research community by MFI material properties, we want to underline that the HP data on the class of zeolites collected and discussed here are still rather incomplete and uneven. Hence, one of the main aims of this review is, beyond describing the state-of-the-art studies on the response to pressure of MFI phases, to make clear that this topic deserves further investigations.

3. MFI materials under pressure

3.1. Elastic behavior and compressibility

The compressibility of a number of MFI materials was studied by *in situ* X-ray powder diffraction (XRPD) or single-crystal XRD, using synchrotron or conventional radiation. All the studies were performed by loading the sample in a diamond–anvil cell (DAC) and compressing the zeolite from P_{amb} to 5–8 GPa, using silicone oil as PTM. The elastic

Table 1
Unit-cell volume variations and elastic parameters K_0 values of the MFI-type zeolites studied in silicone oil (s.o.).

The chemical composition of the studied samples is expressed as the Si/Al ratio, the number of water molecules and the total number of extra-framework electrons obtained from the structure refinements. The elastic parameters of silicalite-1-F (Quartieri *et al.*, 2012) were calculated after the fulfillment of the phase transition to the orthorhombic space group. P_{max}: highest pressure value used in the ΔV% calculation; n.d.: the K_0 value for mutinaite was not calculated due to the low quality of the powder data; n.r.: values not reported in the papers of Haines *et al.* (2009, 2010).

Sample	P_{max} (GPa)	ΔV (%)	K_0 (GPa)	Si/Al ratio	No. of water molecules	No. of extra-framework electrons
Mutinaite[a]	5.97	13.2	n.d.	7.6	60.0	711
H-ZSM-5[b]	6.21	16.6	23.7 (4)	11.4	36.0	379
Na-ZSM-5[c]	6.23	18.5	18.2 (6)	18.3	28.4	343
Silicalite-1-F[a]	6.03	21.2	18.2 (2)	∞	2.5	24
Silicalite-1-OH[a]	6.18	25.4	14.3 (2)	∞	3.0	25
Silicalite-1-F[d]	n.r.	n.r.	13.6 (5) [< 3 GPa] 9.98 (9) [3–8 GPa]	∞	–	n.r.
Silicalite-1-OH[d]	n.r.	n.r.	18.8 (5)	∞	–	n.r.

References: (*a*) Quartieri *et al.* (2012); (*b*) Quartieri *et al.* (2011); (*c*) Arletti *et al.* (2011); (*d*) Haines *et al.* (2009, 2010).

behavior of the following materials (with different framework and extraframework content) are reported in the literature:

(i) Natural mutinaite, chemical formula $(Na_{2.76}K_{0.11}Mg_{0.21}Ca_{3.78})(Al_{11.20}Si_{84.91})\cdot 60H_2O$, Si/Al = 7.6, orthorhombic, space group *Pnma*, with a = 20.201 (2), b = 19.991 (2), c = 13.469 (2) Å (Quartieri *et al.*, 2012).

(ii) Na-ZSM-5, chemical formula $(Na_{4.58}K_{0.02})(Ca_{0.18}Mg_{0.03}Ba_{0.01}Fe_{0.05}Sr_{0.01})(Si_{91.35}Al_{4.48})O_{192}\cdot 28.39H_2O$, Si/Al = 20.4, orthorhombic, space group *Pnma*, a = 20.1359 (1), b = 19.904 (1), c = 13.4363 (9) Å (Arletti *et al.*, 2011).

(iii) H-ZSM-5, chemical formula $(H_{6.8}Na_{1.1})(Al_{7.9}Si_{89.8})O_{192}\cdot 36H_2O$, Si/Al = 11.4, orthorhombic, space group *Pnma*, a = 20.189 (1), b = 19.995 (2), c = 13.460 (1) Å (Quartieri *et al.*, 2011).

(iv) Silicalite-1-OH, prepared by the alkaline route, pure silica (Si/Al ratio equal to infinite); monoclinic space group $P2_1/n$ (Haines *et al.*, 2009, 2010; Quartieri *et al.*, 2012).

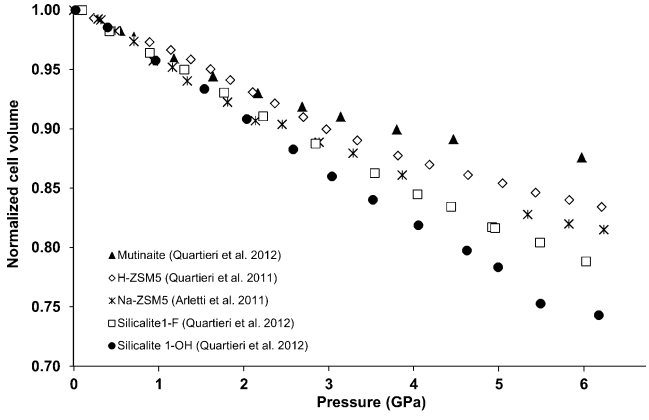

Figure 2
Comparison of the unit-cell volume variations as a function of pressure for mutinaite, H-ZSM5, Na-ZSM5, silicalite A, and silicalite B compressed in silicone oil.

(v) Silicalite-1-F, prepared by the fluoride route, pure silica (Si/Al ratio equal to infinite); monoclinic space group $P2_1/n$ (Haines *et al.*, 2009, 2010; Quartieri *et al.*, 2012).

For all these samples, the P-induced cell parameter variations and the bulk modulus values are reported, while detailed structural information are available only for silicalite-1 (Arletti *et al.*, 2011; Quartieri *et al.*, 2011, 2012). These studies show that, upon decompression, the reversibility of the diffraction peak intensities is only partial, while the original unit-cell parameters are generally recovered. The only exception is silicalite-1, which regains the unit-cell parameters of P_{amb} maintaining the orthorhombic space group assumed at high pressure (Quartieri *et al.*, 2012).

While in mutinaite, H-ZSM-5 and Na-ZSM-5 no high-pressure-induced symmetry change is observed and the original symmetry *Pnma* is maintained upon compression, an irreversible phase transition from the monoclinic $P2_1/n$ to the orthorhombic *Pnma* space group is observed at $\sim$ 1.0 GPa in the silicalite-1 samples.

Table 1 reports the unit-cell volume reduction and the bulk modulus for the MFI materials studied under pressure, together with their Si/Al ratio, the number of H_2O molecules per formula unit (p.f.u.) derived by the chemical analysis, and the total extra-framework content (expressed as the total number of electrons corresponding to both cations and water molecules) derived from the structural refinements. As the bulk modulus values determined for zeolites compressed in 'non-penetrating' media range from $\sim$ 18 to 72 GPa (see for a review Leardini *et al.*, 2010), MFI phases, characterized by K_0 values lower than 20 GPa, can be classified among the most compressible zeolites so far known. Table 1 and Fig. 2 highlight that the phases with the lowest Si/Al ratios, and, as a consequence, the largest extraframework contents, show the lowest unit-cell contractions. The most compressible phases are those with almost empty pores, namely silicalite-1 samples.

In particular, a higher contraction was observed for silicalite-1-OH with respect to silicalite-1-F by Quartieri *et al.* (2012); see Fig. 2. This was ascribed to the significantly higher amount of silanol defects in silicalite-1 synthesized under alkaline conditions with respect to the synthesis in fluoride medium. Haines *et al.* (2009, 2010) attribute the difference between the compressibility of the two silicalites to the non-equilibrium effects achieved during compression, as the silicalite-1-OH was undergoing amorphization, which can give rise to local depressurization. The disagreement among the silicalite-1 bulk modulus values reported by Quartieri *et al.* (2012) and Haines *et al.* (2009, 2010) for the two silicalite-1-OH and the two silicalite-1-F samples, respectively, can be ascribed to both these factors. Specifically, since different

Table 2
Unit-cell parameter variations, elastic parameters K_0 and number of extra-framework sites with additional electrons determined at 1.6 and 2.0 GPa for Na-ZSM-5 and H-ZSM-5 compressed in methanol:ethanol:water (m.e.w.).

The elastic parameters were calculated for both phases above 3.0 GPa, after the end of medium penetration. P_{max}: highest pressure value used in the ΔV% calculation.

Sample	P_{max} (GPa)	Δa (%)	Δb (%)	Δc (%)	ΔV (%)	K_0 (GPa)	No. of additional extra-framework electrons
H-ZSM-5	7.62	5.8	4.8	4.4	14.6	27.5 (6)	104
Na-ZSM-5	7.36	6.3	4.6	4.5	14.6	28.9 (5)	89

synthesis procedures were used in the two studies, it is probable that the silicalite-1 samples investigated by Quartieri *et al.* (2012) and Haines *et al.* (2009, 2010) contain a significantly different amount of silanol defects, able to induce different elastic behaviors. Moreover, the possible presence of a certain amount of amorphous phase in the original silicalite-1-OH used by Haines *et al.* (2009, 2010) could result in a decreased effective value of the applied pressure on the crystalline fraction.

While the most compressible MFI zeolite is silicalite-1, the most rigid material is mutinaite, characterized by the presence of a high number of cations and H_2O molecules p.f.u. in the channels (Vezzalini *et al.*, 1997). All these data confirm that the response to pressure of MFI porous materials is strongly dependent on the extra-framework species, which contribute to stiffen the structure and to contrast the HP-induced channel deformations. In particular, the compressibility increases on increasing the hydrophobic character of the material.

3.2. Pressure-induced hydration and molecule intrusion

The pressure-induced penetration of guest molecules has been investigated in Na- and H-ZSM-5 by synchrotron XRPD experiments up to 1.6 and 2.0 GPa, respectively, using a 16:3:1 methanol:ethanol:water mixture (m.e.w.) as PTM (Arletti *et al.*, 2011; Quartieri *et al.*, 2011).

Table 2 reports the unit-cell parameter variations, the elastic parameter K_0 and the increment of the electrons in the extra-framework sites, determined at 1.6 and 2.0 GPa for Na-HZSM-5 and H-ZSM-5, respectively. The cell volume decrease and the elastic parameters of the two materials are very similar; no phase transitions are observed within the pressure range investigated. The comparison of the data reported in Tables 1 and 2 also shows that the compressibility in m.e.w. is lower than in s.o., indicating a more rigid behavior of these microporous materials when compressed in aqueous media. This was interpreted as due to the penetration of additional PTM molecules. These molecules – corresponding to 89 and 104 additional electrons in the extra-framework sites of Na- and H-ZSM-5, respectively – contrast with the HP-induced structural deformations *via* their interactions with the channel walls. However, the accurate interpretation of this behavior is hindered by the lack of information on the actual total amount of PTM molecules penetrating the two phases under the highest applied pressures. In fact, it cannot be excluded that further PTM molecules penetrate the cavities at a pressure above 2.0 GPa. In Na-ZSM-5 the extra-molecules contribute to increase the occupancy of already existing extra-framework sites (Arletti *et al.*, 2011), while in H-ZSM-5 the guest species occupy both new and already existing sites (Quartieri *et al.*, 2011).

It is worth noting that the increase of the extra-framework content, although extremely high, occurs in both zeolites without any cell volume expansion (Fig. 3). This can be due to the large dimensions of the hosting channels. Actually, PTM penetration in Na-ZSM-5 occurs in the same P range in which a discontinuity in the plot of the unit-cell volume *versus* pressure is observed (at about 2 GPa; Fig. 3). Due to the lack of detailed structural data at high pressure, it cannot be excluded that additional molecules penetrate the structure of Na-ZSM-5 above 1.6 GPa and below 2.9 GPa. Above 3 GPa a strong increase of compressibility is observed (Fig. 3), suggesting that the PTM molecules no longer penetrate the pores and that the pressure exerted on the sample acts directly on the structure deformation.

An interesting difference between H-ZSM-5 and Na-ZSM-5 concerns the reversibility of m.e.w. penetration: while the extra molecules are completely released upon decompression in H-ZSM-5, in Na-ZSM-5 the phenomenon is only partially reversible and hence, in this case, a material with new chemical composition is produced.

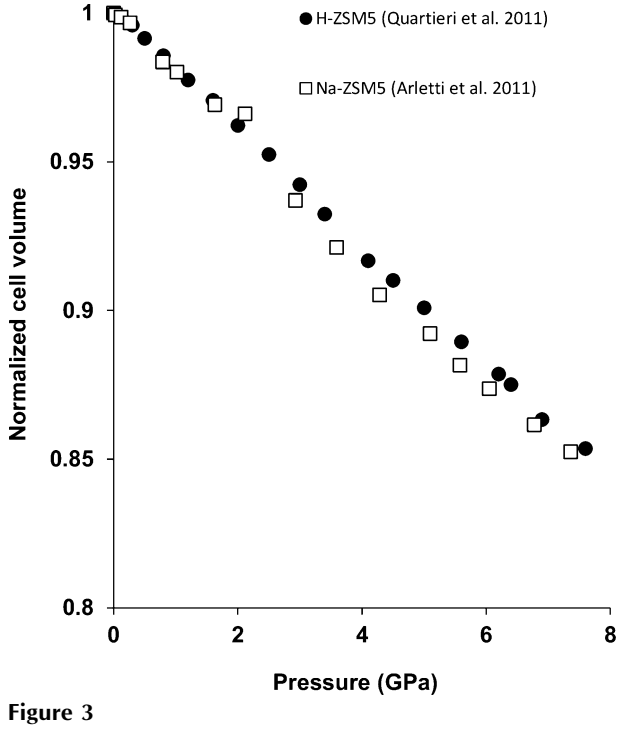

Figure 3
Normalized unit-cell volumes for Na- (empty squares) and H-ZSM-5 (filled circles) as a function of pressure measured in methanol:ethanol:-water (m.e.w.).

Along with the XRPD studies performed in DAC in the pressure regime of GPa, MFI microporous materials have also been studied at lower pressure regimes – combining mercury porosimetry and Gran Canonical Monte Carlo simulations, to verify the spontaneous condensation of water in the nanopores (Desbiens *et al.*, 2005). Both experimental and theoretical data show condensation occurring between 50 and 100 MPa. The observed phenomenon occurs following different steps: at about 50 MPa the condensed fluid is extremely inhomogeneous and the highest water density is found at the intersection between the straight and the zigzag channels, the channels being empty in several sections. Between 50 and 100 MPa, the channel filling becomes more homogenous, even if the highest water density remains at the intersection of the channels. In this way, about 85% of the bulk H_2O density is reached. Finally, above 100 MPa a progressive filling of the pores is observed, with a density at the channel intersection very close to that found for bulk water. As a whole, about 35 H_2O molecules are hosted in the silicalite-1 unit cell at $\sim$ 110 MPa. It has been observed that the presence of defects inside the pores can facilitate a small water uptake at lower pressures, but the real condensation transition is observed at higher pressure. In fact, in a defective silicalite, the isolated 'hydrophilic' patches represented by silanols can act as seeds for water condensation at low pressure, but the last stage of condensation observed in the defect-free part of the pores occurs at higher pressure in a stepwise process (Trzpit *et al.*, 2007). It is worth noting that the intrusion–extrusion process in silicalite-1 is completely reversible and thus this zeolite behaves as a spring, storing and restoring energy. The porous volume of silicalite-1 is increased by the creation of an additional porosity when carbon black is used in the batch during the synthesis in fluoride medium. The formation of a mesoporous phase leads to an increase of the intruded volume at about 100 MPa, and thus to an increase in the amount of stored energy compared with a classical silicalite-1 (+5%).

Since the 'water–silicalite' system behaves as a molecular spring (Karbowiak *et al.*, 2010), the successive intrusion–extrusion cycles of liquid water in small crystallites of hydrophobic silicalite were studied by volumetric and calorimetric techniques. A decrease of the intrusion pressure between the first intrusion–extrusion cycle and the consecutive ones was observed, whereas the extrusion pressure remained unchanged. No structural and morphological modifications of silicalite-1 were observed either by XRD studies or SEM observations. On the contrary, FTIR and solid-state NMR spectroscopic characterizations provided molecular evidence of the chemical modification of the zeolite framework – which occurred during the first water intrusion – with the formation of local silanol defects created by the breaking of siloxane bonds, which can explain a shift in the value of the intrusion pressure in successive cycles.

The penetration of CO_2 in silicalite was investigated by means of Grand Canonical Monte Carlo simulations (Coasne *et al.*, 2011). The authors determined that the average number of adsorbed molecules was 24.5 per unit cell at 3.5 GPa and that CO_2 is preferentially adsorbed in the linear channels running along the *b* direction. A non-negligible adsorption in the sinusoidal channels in the *ac* plane is also observed, in particular at the junction between the linear and sinusoidal channels. The simulated adsorption isotherm showed that the adsorbed molecules increase very sharply in the low pressure range and then reach a plateau as the pores become filled. Upon initial CO_2 adsorption, the unit-cell volume decreases, as a consequence of the interaction of the adsorbed molecules with the zeolite. In contrast, as the encapsulated CO_2 increases, further adsorption requires swelling of the zeolite to accommodate more molecules.

3.3. Pressure-induced amorphization

The recent studies on compressibility of Na-ZSM-5 (Arletti *et al.*, 2011), H-ZSM-5 (Quartieri *et al.*, 2011) and silicalite-1-OH and -F (Quartieri *et al.*, 2012) can shed some light on PIA effects in these materials. In both Na-ZSM-5 and H-ZSM-5 the peak intensities of the HP powder patterns collected in s.o. and m.e.w. decrease and the peak profiles become broader with increasing pressure and this is especially evident in the patterns collected in s.o. These effects can be due to a number of factors: an increase in the long-range structural disorder, or the presence of microstrains caused by deviatoric stress in the quasi-hydrostatic pressure-transmitting medium silicon oil (Fei & Wang, 2000; Lee *et al.*, 2002; Weidner *et al.*, 1998; Yamanaka *et al.*, 1997; Angel *et al.*, 2007). However, no complete PIA is observed, neither in s.o. nor in m.e.w., up to about 8 GPa and the features present in the XRPD patterns collected at P_{amb} in m.e.w. are reversibly regained upon decompression, although the reversibility is only partial for the pattern collected in s.o. In more detail, the HP patterns of the two zeolites collected in m.e.w. are of a higher quality than in s.o. and, among the latter, the patterns of H-ZSM-5 are better than those of the Na form. This can be explained by the stuffing effect of the PTM molecules penetrating during compression, which are in larger number in H-ZSM-5 than in Na-ZSM-5.

Concerning the two silicalite-1 samples studied by Quartieri *et al.* (2012) in s.o. up to 6 GPa, silicalite-1-F appears to be stable up to higher pressure values with respect to silicalite-1-OH. As previously discussed, the higher stability of this species can be attributed to the lower amount of silanol structural defects. Studies performed by Haines *et al.* (2009, 2010) in s.o. report that silicalite-1-OH and silicalite-1-F – after the monoclinic orthorhombic phase transition – undergo a progressive amorphization, which is complete just above 8 GPa. The comparison between the structure of the amorphous form of silicalite-1-F and that of the crystalline phase, performed by Raman spectroscopy, total X-ray scattering, Reverse Monte Carlo (RMC) modeling and PDF analysis, indicated that the amorphous material obtained by PIA retains the basic topology of the initial crystalline phase, but with strong geometrical distortions. This opens the route for preparing new topologically ordered (*i.e.* still retaining the initial chemical bonds and connectivity) amorphous materials with different intermediate range structures, a lower entropy

with respect to a standard glass, and distinct physical and mechanical properties, approaching those of an 'ordered' or 'perfect' (after Greaves *et al.*, 2003) glass (Haines *et al.*, 2009).

When silicalites are compressed in CO_2 or Ar (*i.e.* in penetrating transmitting media) a lower compressibility is observed – with a bulk modulus of 35.9 (4) GPa (Haines *et al.*, 2010), very similar to that of α-quartz (Angel *et al.*, 1997) – and PIA is not observed up to 25 and 22 GPa for silicalite-1-F and silicalite-1-OH, respectively. Furthermore, the Raman spectrum of the recovered silicalite 1-F sample is identical to that of the starting material, confirming the stability of the orthorhombic form in the presence of guest species. This confirms again the crucial role of the molecules adsorbed during compression on the HP behavior of silicalite-1.

The importance of the incorporated molecules on PIA is also discussed by Fu *et al.* (2012), who studied the PIA process of as-made (with template molecules occluded in the zeolite) and calcined Si-pure ZSM-5 by *in situ* Raman spectroscopy and X-ray diffraction, without PTM. These authors demonstrated that, although both phases undergo PIA, their amorphization threshold pressures are different. The pressure values for calcined Si-ZSM-5 are much lower than those for as-made Si-ZSM-5; moreover, calcined Si-ZSM-5 deforms much earlier than the as-made Si-ZSM-5. This is interpreted as due to the lack, in calcined Si-ZSM-5, of the template molecules, which, when present, occupy the 10MR channels. For both zeolites, the LDA phase can be transformed back to the original crystalline MFI structure, but the pressure range for this reversible phase transition is much wider for as-made Si-ZSM-5 (0–7 GPa) than for the calcined one (0–3 GPa), indicating that the TPA^+ cations act as 'organizing centers' to redirect the silica fragments to reform the MFI topology.

Pressure-induced amorphization is also observed when silicalite is compressed in the absence of a PTM, which is in non-hydrostatic conditions. In this case a more gradual peak intensity decrease is observed and the phase undergoes complete amorphization even above 14.6 GPa. A very strong apparent volume increase is observed above 10 GPa, which was justified as a local depressurization effect generated in mixtures of residual crystalline material and amorphous forms of different densities. The local decompression clearly corresponds to a non-equilibrium behavior and, within the powder grains, results in a lower pressure being experienced by the remaining crystallites in the amorphous matrix. Such local depressurization can also justify the persistence, in the absence of PTM, of the crystalline phase up to high pressure. These results can explain the potential shock wave absorption properties of this material, as this local decompression partially 'absorbs' the applied static pressure. A similar apparent volume increase under pressure was previously reported also for zeolite A (Greaves *et al.*, 2003; Greaves & Meneau, 2004) and faujasite (Isambert *et al.*, 2008), even if the effect observed for silicalite-1-F – characterized by empty pores – is particularly marked. It must finally be underlined that the structural stability of loaded silicalite-1 – up to at least 25 GPa – is higher than that observed for the common, non-porous, tetrahedral forms of SiO_2 α-cristobalite and α-quartz, which undergoes a phase transition below this pressure at ambient temperature (Prokopenko *et al.*, 2001; Kingma *et al.*, 1993; Haines *et al.*, 2001). No increase in Si coordination to six is observed in silicalite, in contrast to quartz (Haines *et al.*, 2001).

This work was supported by the Italian MIUR, in the frame of the following projects: PRIN2009 'Struttura, microstruttura e proprietà dei minerali'; PRIN2010-11 'Dalle materie prime del sistema Terra alle applicazioni tecnologiche: studi cristallochimici e strutturali'; FIRB, Futuro in Ricerca 'Impose Pressure and Change Technology' (RBFR12CLQD).

References

Angel, R. J., Allan, D. R., Miletich, R. & Finger, L. W. (1997). *J. Appl. Cryst.* **30**, 461–466.
Angel, R. J., Bujak, M., Zhao, J., Gatta, G. D. & Jacobsen, S. D. (2007). *J. Appl. Cryst.* **40**, 26–32.
Argauer, R. J. & Landolt, G. R. (1972). US Patent 3, 702 886.
Arletti, R., Ferro, O., Quartieri, S., Sani, A., Tabacchi, G. & Vezzalini, G. (2003). *Am. Mineral.* **88**, 1416–1422.
Arletti, R., Quartieri, S. & Vezzalini, G. (2010). *Am. Mineral.* **95**, 1247–1256.
Arletti, R., Vezzalini, G., Morsli, A., Di Renzo, F., Dmitriev, V. & Quartieri, S. (2011). *Microporous Mesoporous Mater.* **142**, 696–707.
Artioli, G., Lamberti, C. & Marra, G. L. (2000). *Acta Cryst.* B**56**, 2–10.
Baerlocher, Ch., Meier, W. M. & Olson, D. H. (2001). *Atlas of Zeolite Framework Types.* Amsterdam: Elsevier.
Belitsky, I. A., Fursenko, B. A., Gabuda, S. P., Kholdeev, O. V. & Seryotkin, Y. V. (1992). *Phys. Chem. Miner.* **18**, 497–505.
Betti, C., Fois, E., Mazzucato, E., Medici, C., Quartieri, S., Tabacchi, G., Vezzalini, G. & Dmitriev, V. (2007). *Microporous Mesoporous Mater.* **103**, 190–209.
Cailliez, F., Boutin, A., Demachy, I. & Fuchs, A. H. (2009). *Mol. Simul.* **35**, 24–30.
Cailliez, F., Trzpit, M., Soulard, M., Demachy, I., Boutin, A., Patarin, J. & Fuchs, A. H. (2008). *Phys. Chem. Chem. Phys.* **10**, 4817–4826.
Chelazzi, D., Ceppatelli, M., Santoro, M., Bini, R. & Schettino, V. (2004). *Nat. Mater.* p. 3.
Citroni, M., Ceppatelli, M., Bini, R. & Schettino, V. (2002). *Science*, **295**, 2058–2060.
Coasne, B., Haines, J., Levelut, C., Cambon, O., Santoro, M., Gorelli, F. & Garbarino, G. (2011). *Phys. Chem. Chem. Phys.* **13**, 20096–20099.
Colligan, M., Forster, P. M., Cheetham, A. K., Lee, Y., Vogt, T. & Hriljac, J. A. (2004). *J. Am. Chem. Soc.* **126**, 12015–12022.
Cundy, C. S. & Cox, P. A. (2003). *Chem. Rev.* **103**, 663–702.
Demontis, P., Stara, G. & Suffritti, G. B. (2003). *J. Phys. Chem. B*, **107**, 4426–4436.
Desbiens, N., Demachy, I., Fuchs, A. H., Kirsch-Rodeschini, H., Soulard, M. & Patarin, J. (2005). *Angew. Chem. Int. Ed.* **44**, 5310–5313.
Eissmann, R. N. & LeVan, M. D. (1993). *Ind. Eng. Chem. Res.* **32**, 2752–2757.
Eroshenko, V., Regis, R. C., Soulard, M. & Patarin, J. (2001). *J. Am. Chem. Soc.* **123**, 8129–8130.
Eroshenko, V., Regis, R. C., Soulard, M. & Patarin, J. (2002). *C. R. Phys.* **3**, 111–119.
Fadeev, A. Y. & Eroshenko, V. A. (1997). *J. Colloid Interface Sci.* **187**, 275–282.
Fei, Y. & Wang, Y. (2000). *High-Pressure, High-Temperature Crystal Chemistry. Reviews in Mineralogy and Geochemistry*, edited by R. M. Hazen & R. T. Downs, pp. 41, 521–557. The Mineralogical Society of America and the Geochemical Society, Washington DC, USA.

Flanigen, E. M., Bennett, J. M., Grose, R. W., Cohen, J. P., Patton, R. L., Kirchner, R. M. & Smith, J. V. (1978). *Nature*, **271**, 512–516.
Fois, E., Gamba, A., Medici, C., Tabacchi, G., Quartieri, S., Mazzucato, E., Arletti, R., Vezzalini, G. & Dmitriev, V. (2008). *Microporous Mesoporous Mater.* **115**, 267–280.
Fois, E., Gamba, A., Tabacchi, G., Arletti, R., Quartieri, S. & Vezzalini, G. (2005). *Am. Mineral.* **90**, 28–35.
Fois, E., Gamba, A., Tabacchi, G., Quartieri, S., Arletti, R. & Vezzalini, G. (2005). *Studies In Surface Science and Catalysis*, edited by A. Gamba, Vol. 155, pp. 271–280. Amsterdam: Elsevier Science.
Fu, Y., Song, Y. & Huang, Y. (2012). *J. Phys. Chem. C*, **116**, 2080–2089.
Galli, E., Vezzalini, G., Quartieri, S., Alberti, A. & Franzini, M. (1997). *Zeolites*, **18**, 318–322.
Gatta, G. D. (2005). *Eur. J. Mineral.* **17**, 411–422.
Gatta, G. D. (2008). *Z. Kristallogr.* **223**, 160–170.
Gillet, P., Malezieux, J. & Itie, J. (1996). *Am. Mineral.* **81**, 651–657.
Goryainov, S. V. (2005). *Phys. Status Solidi*, **202**, R25–R27.
Goryainov, S. V., Fursenko, B. A. & Belitsky, I. A. (1996). *Phys. Chem. Miner.* **23**, 297–308.
Goryainov, S. V., Kurnosov, A. V., Miroshnichenko, Y. M., Smirnov, M. B. & Kabanov, I. S. (2003). *Microporous Mesoporous Mater.* **61**, 283–289.
Goryainov, S. V. & Smirnov, M. B. (2001). *Eur. J. Mineral.* **13**, 507–519.
Greaves, N. & Meneau, F. (2004). *J. Phys. Condens. Matter*, **16**, S3459–S3472.
Greaves, G. N., Meneau, F., Sapelkin, A., Colyer, L. M., Gwynn, I. A., Wade, S. & Sankar, G. (2003). *Nat. Mater.* **2**, 622–629.
Gulín-González, J. & Suffritti, G. B. (2004). *Microporous Mesoporous Mater.* **69**, 127–134.
Haines, J., Cambon, O., Levelut, C., Santoro, M., Gorelli, F. & Garbarino, G. (2010). *J. Am. Chem. Soc.* **132**, 8860–8861.
Haines, J., Léger, J. M., Gorelli, F. & Hanfland, M. (2001). *Phys. Rev. Lett.* **87**, 155503.
Haines, J., Levelut, C., Isambert, A., Hébert, P., Kohara, S., Keen, D. A., Hammouda, T. & Andrault, D. (2009). *J. Am. Chem. Soc.* **131**, 12333–12338.
Havenga, E. A., Huang, Y. & Secco, R. A. (2003). *Mater. Res. Bull.* **38**, 381–387.
Hay, D. G. & Jaeger, H. (1984). *J. Chem. Soc. Chem. Commun.* p. 1433.
Huang, Y. J. (1998). *Mater. Chem.* **8**, 1067–1071.
Huang, Y. & Havenga, E. A. (2001). *Chem. Phys. Lett.* **345**, 65–71.
Isambert, A., Angot, E., Hébert, P., Haines, J., Levelut, C., Le Parc, R., Ohishi, Y., Kohara, S. & Keen, D. A. (2008). *J. Mater. Chem.* **18**, 5746–5752.
Karbowiak, T., Saada, M. A., Rigolet, S., Ballandras, A., Weber, G., Bezverkhyy, I., Soulard, M., Patarin, J. & Bellat, J. P. (2010). *Phys. Chem. Chem. Phys.* **12**, 11454–11466.
Kingma, K. J., Hemley, R. J., Mao, H. K. & Veblen, D. R. (1993). *Phys. Rev. Lett.* **70**, 3927–3930.
Kokotailo, G. T., Lawton, S. L., Olson, D. H. & Meier, W. M. (1978). *Nature*, **272**, 437–438.
Koningsveld, H. van, Jansen, J. C. & van Bekkum, H. (1987). *Zeolites*, **7**, 564–568.
Leardini, L., Quartieri, S., Martucci, A., Vezzalini, G. & Dmitriev, V. (2012). *Z. Kristallogr.* **227**, 514–521.
Leardini, L., Quartieri, S. & Vezzalini, G. (2010). *Microporous Mesoporous Mater.* **127**, 219–227.
Leardini, L., Quartieri, S., Vezzalini, G., Martucci, A. & Dmitriev, V. (2013). *Microporous Mesoporous Mater.* **170**, 52–61.
Lee, Y., Hriljac, J. A., Studer, A. & Vogt, T. (2004). *Phys. Chem. Miner.* **31**, 22–27.
Lee, Y., Kao, C., Kim, S. J., Lee, H., Lee, D. R., Shin, T. J. & Choi, J. (2007). *Chem. Mater.* **19**, 6252–6257.
Lee, Y., Vogt, T., Hriljac, J. A., Parise, J. B. & Artioli, G. (2002). *J. Am. Chem. Soc.* **124**, 5466–5475.
Likhacheva, A. Yu., Seryotkin, Y. V., Manakov, A., Goryainov, S. V. & Ancharov, A. I. (2006). *Z. Kristallogr.* **224**, 37–143.
Likhacheva, A. Y., Seryotkin, Y. V., Manakov, A. Y., Goryainov, S. V., Ancharov, A. I. & Sheromov, M. A. (2007). *Am. Mineral.* **92**, 1610–1615.
Lok, B. M., Cannan, T. R. & Messina, C. A. (1983). *Zeolites*, **3**, 282–291.
Lui, H., Secco, R. A. & Huang, Y. (2001). *Phys. Chem. Commun.* **8**, 1–3.
Martin, T., Lefevre, B., Brunel, D., Galarneau, A., Di Renzo, F., Fajula, F., Gobin, P. F., Quinson, J. F. & Vigier, G. (2002). *Chem. Commun.* **2002**, 24–25.
Miroshnichenko, Y. M. & Goryainov, S. V. (2000). *Mineral. Mag.* **64**, 301–309.
Olson, D. H., Kokotailo, G. T., Lawton, S. L. & Meier, W. M. (1981). *J. Phys. Chem.* **85**, 2238–2243.
Ori, S., Quartieri, S., Vezzalini, G. & Dmitriev, V. (2008). *Am. Mineral.* **93**, 1393–1403.
Peral, I. & Iñiguez, J. (2006). *Phys. Rev. Lett.* **97**, 225502.
Prokopenko, V. B., Dubrovinsky, L. S., Dmitriev, V. & Weber, H. P. J. (2001). *Alloys Compd.* **327**, 87–95.
Quartieri, S., Arletti, R., Vezzalini, G., Di Renzo, F. & Dmitriev, V. (2012). *J. Solid State Chem.* **191**, 201–212.
Quartieri, S., Montagna, G., Arletti, R. & Vezzalini, G. (2011). *J. Solid State Chem.* **184**, 1505–1516.
Richet, P. & Gillet, P. (1997). *Eur. J. Mineral.* **9**, 907–933.
Rutter, M. D., Secco, R. A. & Huang, Y. (2000). *Chem. Phys. Lett.* **331**, 189–195.
Rutter, M. D., Uchida, T., Secco, R., Huang, Y. & Wang, Y. (2001). *J. Phys. Chem. Solids*, **62**, 599–606.
Santoro, M., Gorelli, F. A, Bini, R., Haines, J. & van der Lee, A. (2013). *Nat. Commun.* **4**, 1557.
Sartbaeva, A., Haines, J., Cambon, O., Santoro, M., Gorelli, F., Levelut, C., Garbarino, G. & Wells, S. A. (2012). *Phys. Rev. B*, **85**, 064109.
Sartbaeva, A., Wells, S. A., Treacy, M. M. & Thorpe, M. F. (2006). *Nat. Mater.* **5**, 962–965.
Schettino, V. & Bini, R. (2003). *Phys. Chem. Chem. Phys.* **5**, 1951–1965.
Secco, R. A. & Huang, Y. (1999). *J. Phys. Chem. Solids*, **60**, 999–1002.
Seryotkin, Y. V., Bakakin, V. V., Fursenko, B. A., Belitsky, I. A., Joswig, W. & Radaelli, P. G. (2005). *Eur. J. Miner.* **17**, 305–314.
Sharma, S. M. & Sikka, S. K. (1996). *Prog. Mater. Sci.* **40**, 1–77.
Soulard, M., Patarin, J., Eroshenko, V. & Regis, R. C. (2004). *Proceedings of the 14th International Zeolite Conference 2003*, p. 1830. Cape Town, South Africa.
Stelzer, J., Paulus, M., Hunger, M. & Weitkamp, J. (1998). *Microporous Mesoporous Mater.* **22**, 1–8.
Trzpit, M., Rigolet, S., Paillaud, J. L., Marichal, C., Soulard, M. & Patarin, J. (2008). *J. Phys. Chem. B*, **112**, 7257–7266.
Trzpit, M., Soulard, M. & Patarin, J. (2009*a*). *J. Mater. Sci.* **44**, 6525–6530.
Trzpit, M., Soulard, M. & Patarin, J. (2009*b*). *Microporous Mesoporous Mater.* **117**, 627–634.
Trzpit, M., Soulard, M., Patarin, J., Desbiens, N., Cailliez, F., Boutin, A., Demachy, I. & Fuchs, A. H. (2007). *Langmuir*, **23**, 10131–10139.
Vezzalini, G., Quartieri, S., Galli, E., Alberti, A., Cruciani, G. & Kvick, A. (1997). *Zeolites*, **19**, 323–325.
de Vos Burchart, E., van Bekkum, H. & van de Graaf, B. (1993). *Zeolites*, **13**, 212–215.
Washburn, E. W. (1921). *Proc. Natl Acad. Sci. USA*, **7**, 115–116.
Weidner, D. J., Huang, Y., Chen, G., Hando, J. & Vaughan, M. T. (1998). *Properties of Earth and Planetary Materials at High Pressure and Temperature*, edited by M. H. Manghnani & T. Yagy, pp. 473–480. Washington, DC: American Geophysics Union.
Yamanaka, T., Nagai, T. & Tsuchiya, T. (1997). *Z. Kristallogr.* **212**, 401–410.